Journal of the Korean Nuclear Society
Volume 26, Number 2, June 1994

Dynamic Stability of a Flexible Cylinder Subjected to Inviscid Flow in a Coaxial Cylindrical Duct Based on Spectral Method

Woo Gun Sim and Yoon Yeong Bae
Korea Atomic Energy Research Institute
(Received November 13, 1993)

스펙트럼 배치방법에 의한 원형도관내의 비점성유동장에 놓인 유연성 실린더의 안정성 분석

심우건 · 배윤영
한국원자력연구소
(1993. 11. 13 접수)

Abstract

A numerical method has been developed for studying the dynamics of a flexible cylinder in a coaxial cylindrical duct, immersed in inviscid flow. The unsteady inviscid fluid-dynamic force acting on the oscillating cylinder has been estimated more rigorously by means of a spectral collocation method without simplification of governing equations. This numerical approach is applicable to the system having wider annular gap and/or shorter length of cylinder as compared to existing potential theory. The governing equation of the unsteady flow was obtained from Laplace equation. The equation of cylinder motion coupled with the fluid motion was discretized by Galerkin's method, from which the dynamic behaviour of the system has been evaluated. The effect of the length of the cylinder and the annular gap on the critical flow velocity, where the system loses stability by buckling, was investigated. To validate the numerical method, the potential flow theory developed by Hobson based on thin film approximation has been improved. Typical results of the present numerical theory on the dynamics and stability of the system are compared with those of available existing theory and the present approximate results. Good agreement was found between the results. It was also found that a nondimensional critical flow velocity becomes larger as increasing the annular gap and decreasing the length of cylinder.

요 약

원형도관내의 비점성유동장에 놓인 동심인 유연성 실린더의 안정성을 분석하기 위하여 수치해석적방법이 개발되었다. 진동하는 실린더에 작용하는 비정상 · 비점성 유체유발력을 스펙트럼 배치방법을 사용하여 지배방정식을 단순화시키지 않음으로서 더 정밀하게 예측하였다. 본 수치해석이론은 기존의 퍼텐샬이론과 비해 비교적 넓은 환의 경우와 짧은 실린더의 경우에도 적용할 수 있다. 비점성유동의 지배방정식은 라플라스방정식으로부터 구하였다. 유체유동과 결부된 실린더의 유동방정식은 갤러킨의 방법에 의하여 불연속방정식으로 표시되며 이로부터 계의 운동특성을 검토하였다. 계가 좌굴현상에 의하여 안

정성을 잃는 임계유속에 대한 환의 간격과 실린더의 길이의 영향이 검토되었다. 수치해석방법을 입증하기 위하여 얇은 막 근사이론에 근거를 두고 호프슨이 제안한 퍼텐샬이론을 개선하였다. 계의 안정성과 동적특성을 수치해석방법에 의하여 예시하였고 기존의 이론과 본 연구에서 제안된 근사법으로 구한 결과와 비교하여 잘 일치함을 보였다. 무차원화된 임계유속은 환의 간격이 넓을수록 실린더의 길이가 짧을수록 증가함을 보였다.

1. Introduction

In recent years, the dynamics of cylindrical beam in axial annular flow has been studied theoretially and experimentally, to evaluate the coupling effects of flow on critical flow velocity[1-3] where the system loses stability. The flow-induced vibration problem has been arisen in nuclear and other industrial plants where damages due to wear, fatigue and fracture of components have been occurred. The natures of the added mass, fluid damping and fluidelastic forces generated by oscillatory motion in annulus are of particular interest to the field of heat exchanger and nuclear reactor components design. An excellent review on flow-induced vibration in nuclear reactor and heat exchanges is given by Paidoussis[4].

During refuelling of PWR type of nuclear reactor shown in Figure 1(a), several holes (wear penetrations) at the guide tube were discovered. The wear occurs at the top of the guide tubes adjacent to the tips of the control rod in their fully withdrawn position, where they normally remain most of time. Similarly, flow in the annular diffusing section provides the main source of detrimental excitation during on-load refuelling of the AGR type of nuclear reactor shown in Figure 1(b).

It may be an essential requirement to understand the mechanism of self-excited vibration, in order to develop analytical methods and give guidelines for designing heat exchangers and nuclear reactor components. As the first step toward satisfying this requirement, the potential flow theory is developed in the present analysis. When the cylinder oscillates with very high frequency and/or in relatively low viscous fluid, the ratio of penetration depth to annular gap is very small. In this case, the fluid-dynamic forces can be estimated by potential flow theory. In the present analysis, the critical flow velocity is estimated by potential theory based on spectral collocation method[5]. In general, the critical flow velocity calculated by potential flow theory is overestimated. In other words, viscous effects stabilize the system, becoming more important as the annulus becomes narrower, which is reasonable on physical grounds. It was also found that, for wide annulus, the viscous effect on the fluid-dynamic forces can be negligible. In contrast to previous works, the present model is applicable to relatively wide annulus and to cylinders of small length-to-radius ratio, which is one of the main contributions of this paper.

The first analytical study for the coaxial cylindrical bodies was undertaken by Hobson[6]. For simplicity, the model was formulated by considering a rigid cylindrical body, hinged at one point. Based on thin film approximation to annulus, radial velocity and radial variation of velocity were neglected and radial variation in pressure was ignored. The approximate model was capable of dealing with situations of sudden contraction or enlargement in the flow passage in some degree of empiricism. A more rigorous, purely analytical study but for very narrow annular flow was accomplished for a rigid body hinged at one point by Mateescu and Paidoussis[7, 8]. The latter model was subsequently extended to take into account stability of flexible cylinder coaxially mounted in a flow-carrying conduit[9]. These analytical models are mainly based on restrictive assumption and simplified flow model. However, despite the success of these simplified solutions, it is obviously necessary to develop more accurate formulation. In this respect, the present analysis based on spectral method was developed by authors (Mateescu, Paidoussis and Sim) to

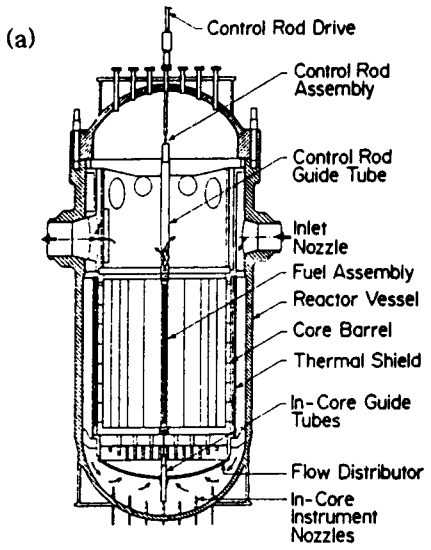

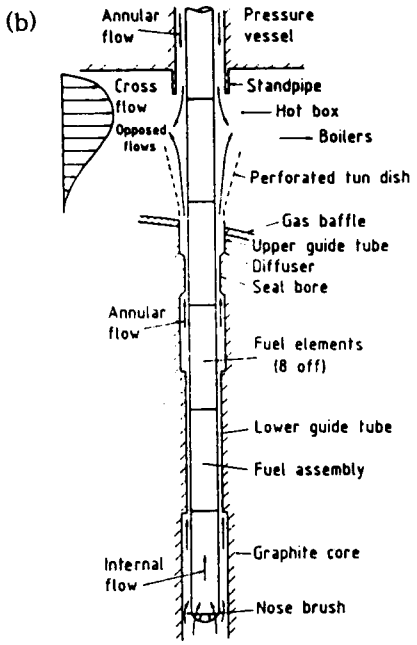

Fig. 1. Annular-flow-induced Vibration (a) between Control Rods and Guide Tube of PWR Nuclear Reactor and (b) between Fuel Assembly and channel of AGR Nuclear Reactor.

estimate hydrodynamic forces acting on a flexible cylinder for concentric configurations[10].

The principal objective of the present work is to develop new and/or improved method to avoid detrimental flow-induced vibration. To achieve this objective, a numerical approach with spectral method, which is an extension of an earlier theory[10], is adapted to study dynamic stability of a flexible cylinder subjected to inviscid annular flow. Based on thin film approximation the potential flow theory developed by Hobson is further refined. By both method, the effect of length of cylinder on the dynamics and stability of system has been evaluated through a five-mode Galerkin's discretization of system. For validation of the spectral method, the numerical solution is compared with previous results and the present approximate solution.

2. Problem Formulation

2.1. General Consideration

The system considered in the present analysis consists of a flexible cylindrical centre-body coaxially mounted in a flow-carrying conduit. The flexible part of the centre-body has length L and both ends of a flexible part of the centre-body are supposed to be clamped, as shown in Figure 2. The flexible centre-body with radius a is free to oscillate in flexure. This system is coupled, by the fluid-dynamic force, due to the inviscid annular flow.

Far upstream, the annular flow is assumed to be steady and is characterized by mean flow velocity U, the static pressure P_∞ and the density ρ, which is considered constant. The time dependent lateral displacement $e_0(x, t)$ of the centre-body axis is assumed to be small with respect to its radius, which permits to use linear theory for the flexural oscillation of the centre-body; hence, i) no separation occurs in the annular flow, and ii) the fluid-dynamic forces acting on each element of the flexible centre-body may be determined using a convenient linearization of the

aerodynamic boundary conditions on the oscillating centre-body. This also means that the assumption of small amplitude oscillation can be utilized in the inviscid analysis of the unsteady fluid-dynamic problem.

To calculate the fluid-dynamic forces acting on a cylinder surrounded by an inviscid flow, the spectral collocation method was applied to system. Detail of this analysis, which remains the same as shown in the previous study[10], are omitted here.

2.2. The Equation of Cylinder Motion

The oscillating flexible centre-body is considered as Euler-Bernoulli beam characterized by flexural rigidity EI, cross-sectional area A_s, length L and density ρ_s. The cylinder under consideration has radius a and the annular gap is H, hence the radius of the conduit is $a_d = a + H$. The circular frequency of the flexible cylinder is denoted by Ω.

The derivation of the equation of small lateral motions is obtained by considering the equilibrium of forces acting on a differential segment of the flexible centre-body based on Hamilton's principle. Therefore, the equation of motion of the flexible centre-body is expressed, as follows:

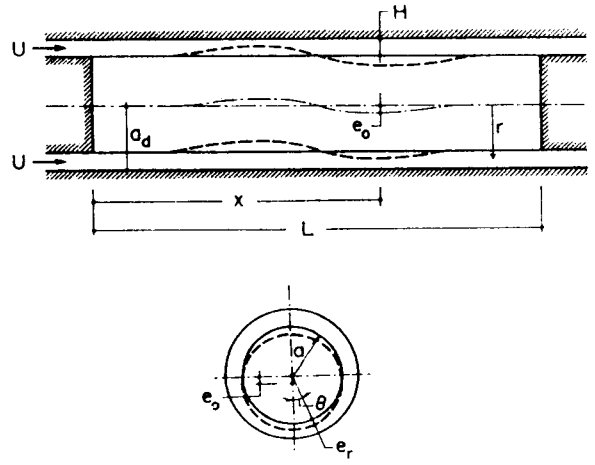

Fig. 2. Geometry of the Flexible Centre-body Oscillating in a Duct with Annular Flow.

$$EI\frac{\partial^4 e_o}{\partial x^4} + \rho_s A_s \frac{\partial^2 e_o}{\partial t^2} = F_p, \tag{1}$$

where $F_p(x, t)$ is the unsteady potential fluid force acting on oscillating cylinder per unit length. The first and the second term of the left-hand side of the above equation may be interpreted physically as the flexible restoring force and the beam inertia force, respectively. The task ahead in the following section is to derive the inviscid force, F_p. The radial displacement at azimuthal direction θ may be written as

$$e_r(x,\theta,t) = e_o(x,t)\cos\theta = E(x)\cos\theta\, e^{i\omega t} \tag{2}$$

In the present analysis, E(x) could be clearly expressed in terms of eigenfunctions, $E_k(x)$, of a beam with the same boundary conditions as the cylinder clamped at both ends. For future purpose, it is more convenient to separate these eigenfunctions into two components, one trigonometric, $E_{1k}(x)$, and the other hyperbolic, $E_{2k}(x)$; thus,

$$E(x) = \sum_k E_k(x) = \sum_k \sum_{s=1}^{2} a_k E_{sk}(x) \tag{3}$$

where

$$\begin{aligned} E_{1k}(x) &= -\cos(\beta_k x/L) + \sigma_k \sin(\beta_k x/L) \\ E_{2k}(x) &= \cosh(\beta_k x/L) - \sigma_k \sinh(\beta_k x/L) \end{aligned} \tag{4}$$

and $\sigma_k = [\cosh(\beta_k) - \cos(\beta_k)]/[\sinh(\beta_k) - \sin(\beta_k)]$, the β_k being the corresponding eigenvalues.

In order to generalize the equation of the motion of the system, it is convenient to define the following dimensionless parameters:

$$\begin{aligned} &\eta = \frac{e_o}{a},\ X = \frac{x}{L},\ l = \frac{L}{a},\ H = \frac{H}{a}, \\ &\tilde{u} = \frac{u^*}{U},\quad \tilde{w} = \frac{w^*}{U},\quad \tilde{p} = \frac{p^*}{\rho U^2}, \\ &U_r = \frac{U}{U_{ref}},\quad U_{ref} = \left(\frac{EI}{\rho_s A_s L^2}\right)^{1/2}, \\ &U_{r1} = \frac{U}{U_{ref1}},\quad U_{ref1} = \left(\frac{EI}{\rho A_s L^2}\right)^{1/2}, \\ &\tilde{t} = \frac{U_{ref}}{L}t,\quad \omega = \frac{\Omega L}{U_{ref}},\quad \sigma = \frac{\rho \pi L^2}{\rho_s A_s}. \end{aligned} \tag{5}$$

2.3. Determination of the Inviscid Forces

In the present analysis, the flow is presumed to be irrotational and incompressible in addition to being

inviscid, so that Laplace equation derived from the continuity equation and momentum equation is reduced to Bernoulli-Lagrange equation. The equation of the unsteady potential flow will be briefly discussed here, and then adapted to the problem at hand, namely to the case of a flexible cylindrical centre-body. A quite different analytical approach to the numerical one has been developed by an adaptation of thin film approximation. To derive the governing equation, momentum fluxes on a small element of annulus are considered.

The inviscid fluid-dynamic forces acting on the centre-body per unit length are determined by integrating the unsteady pressure:

$$F_p(x,t) = -\int_0^{2\pi} a(p-P_\infty)\,|_{r=a}\cos\theta\, d\theta, \qquad (6)$$

where $p(x, \theta, t) = P_\infty + p^*(x)\cos\theta\, e^{i\Omega t}$ as defined in equation (22). As a result, the fluid-dynamic forces may be written as

$$F_p = -\rho\pi a^2 e^{i\Omega t}\sum_k a_k\,(-\Omega^2 P_{2k} + i\Omega P_{1k} + P_{0k}), \qquad (7)$$

where each of the P_{jk} associated with the jth time derivative will be determined later. Physically, P_{2k} is the component associated with inertial effects, P_{1k} with damping effects and P_{0k} with stiffness effects.

2.3.1. Numerical Solution Based on Spectral Method

Under considerations, the inviscid forces are derived by potential flow theory. The velocity potential, $\Phi(x, r, \theta, t)$, must satisfy the Laplace equation

$$\nabla^2\Phi = \frac{\partial^2\Phi}{\partial x^2} + \frac{\partial^2\Phi}{\partial r^2} + \frac{1}{r}\frac{\partial\Phi}{\partial r} + \frac{1}{r^2}\frac{\partial^2\Phi}{\partial\theta^2} = 0, \qquad (8)$$

subjected to the boundary conditions, which imply that the normal velocities of the body are equal to those of the fluid at the boundary surface between the fluid and the body, as follows:

$$\frac{\partial f_b}{\partial t} + V\cdot\nabla f_b = 0, \qquad (9)$$

where V denotes the velocity vector of flow at a point of the free surface and f_b is the equation of the solid-fluid surface written as

$$f_b = r - a - e_r(x,\theta,t) \quad \text{for oscillating body,}$$
$$f_b = r - a - H \quad \text{for fixed body.} \qquad (10)$$

The velocity potential may be written as

$$\Phi(x,r,\theta,t) = \phi_s(x) + \phi(x,r,\theta,t), \qquad (11)$$

the sum of steady and unsteady components.

Following the cited reference[10], the velocity potential may be written in the form

$$\phi = \sum_k a_k\,\hat{\phi}_k(x,r)\cos\theta\, e^{i\Omega t}, \qquad (12)$$

where, by separation of variables, the reduced potentials, $\hat{\phi}_k(x, r)$, may be expressed in terms of the new coordinate, Z, obtained by coordinate transformation, $Z = 1 - 2(r-a)/H$, in the form

$$\hat{\phi}_k(x,Z) = \sum_{s=1}^{2} f_{sk}(x)F_{sk}(Z) = \hat{\phi}_{1k}(x,Z) + \hat{\phi}_{2k}(x,Z). \qquad (13)$$

In the above equation, the reduced potentials can be separated into trigonometric and hyperbolic components (related to the eigenfunctions of the oscillating beam with fixed ends - see equations (3) – (4), as follows:

$$\hat{\phi}_{1k}(x,Z) = [A_a\cos\beta_k x + A_b\sin\beta_k x]\sum_j \Phi_{1kj}T_j(Z),$$
$$\hat{\phi}_{2k}(x,Z) = [B_a\cosh\beta_k x + B_b\sinh\beta_k x]\sum_j \Phi_{2kj}T_j(Z). \qquad (14)$$

In the present spectral approach, Chebyshev polynomials are used for $T_j(Z)$ and the a priori unknown coefficients, Φ_{skj}, will be determined by collocation method.

Taking into account the coordinate transformation, the governing equation (8) may be expressed in terms of reduced potential as

$$\frac{H^2}{4}\frac{\partial^2\hat{\phi}_k}{\partial x^2} + \frac{\partial^2\hat{\phi}_k}{\partial Z^2} - \sqrt{D}\frac{\partial\hat{\phi}_k}{\partial Z} - D\hat{\phi}_k = 0, \qquad (15)$$

where $D = [H/\{2 + (1-Z)H\}]^2$ with boundary condition (10), to be writteen as

$$\frac{\partial\hat{\phi}_k}{\partial Z}|_{Z=-1} = 0,$$
$$\frac{\partial\hat{\phi}_k}{\partial Z}|_{Z=1} = -\frac{H}{2}[i\Omega E_k(x) + UE_k'(x)], \qquad (16)$$

where the prime denotes differentiation with respect to x. Since $\phi(x, r, \theta, t)$ satisfies Laplace equation, the following equations define the trigonometric (s = 1) and hyperbolic (s = 2) components of the reduced potentials

$$\sum_{j=0}^{m}[\Phi_{skj}T_j''(Z) - \sqrt{D}\Phi_{skj}T_j'(Z) - \{D\pm(\frac{H\beta_k}{2})^2\}\Phi_{skj}T_j(Z)] = 0, \quad (17)$$

subject to boundary conditions

$$\sum_{j=0}^{m}\sum_{s=1}^{2}f_{sk}(x)\Phi_{skj}T_j'(-1) = 0,$$
$$\sum_{j=0}^{m}\sum_{s=1}^{2}f_{sk}(x)\Phi_{skj}T_j'(1) = -\frac{H}{2}\sum_{s=1}^{2}[\iota\Omega E_{sk}(x) + UE_{sk}'(x)], \quad (18)$$

through which the constants, A_a, A_b, B_a and B_b, are determined, by separating the boundary conditions in to the trigonometric and hyperbolic components, as

$$A_a = -\frac{H}{2}[-\iota\Omega + U\sigma_k\beta_k],$$
$$A_b = -\frac{H}{2}[\iota\Omega\sigma_k - U\beta_k],$$
$$B_a = -\frac{H}{2}[\iota\Omega - U\sigma_k\beta_k],$$
$$B_b = -\frac{H}{2}[-\iota\Omega\sigma_k + U\beta_k]. \quad (19)$$

The *a priori* unknown coefficients Φ_{skj} are determined from the system of equations obtained by imposing equation (17) on (m-1) collocation points equally distributed in the radial direction and the boundary conditions (18) and the solution of the reduced potential can be completely determined from algebraic equation obtained. Thus the reduced potential can be evaluated on the surface of the moving cylinder:

$$\hat{\phi}_k(x,1) = -\sum_{s=1}^{2}G_{sk}[\iota\Omega E_{sk}(x) + UE_{sk}'(x)] \quad (20)$$

where

$$G_{1k} = \frac{H}{2}\sum_{j=0}^{m}\Phi_{1kj}, \quad G_{2k} = \frac{H}{2}\sum_{j=0}^{m}\Phi_{2kj} \quad (21)$$

The perturbation pressure in the unsteady potential flow can be determined from the Bernoulli-Lagrange equation after suitable linearization,

$$p - P_\infty = \frac{1}{2}\rho U^2 - \frac{1}{2}\rho|\nabla(\phi_s+\phi)|^2 - \rho\frac{\partial\phi}{\partial t}. \quad (22)$$

Hence, the force on the cylinder may be obtained by equation (6) through which the components (P_{2k} associated with inertial effects, P_{1k} with damping effects and P_{0k} with stifness effects) are given by

$$P_{2k} = \sum_{s=1}^{2}G_{sk}E_{sk}(x), \quad P_{1k} = 2U\sum_{s=1}^{2}G_{sk}E_{sk}'(x),$$
$$P_{0k} = U^2\beta_k^2\sum_{s=1}^{2}(-1)^s G_{sk}E_{sk}(x). \quad (23)$$

By inspection of the above equation, it is obvious that P_{1k} and P_{0k} are related to Coriolis and centrifugal forces, respectively.

2.3.2. Analytical Solution Based on Thin Film Approximation

The unsteady equation is derived by assuming a thin film approximation in annulus, from which radial velocity and radial variations of velocities and pressure might be ignored. Based on small amplitude of oscillating motion, the governing equation can be linearized. Solution of the equation will be facilitated by assuming a sine/cosine variation of variable including annular width, in circumferential direction. Thus the variables may vary as

$$h(x,\theta,t) = H + E(x)\cos\theta\, e^{\iota\omega t},$$
$$u(x,\theta,t) = U + u^*(x)\cos\theta\, e^{\iota\omega t},$$
$$w(x,\theta,t) = w^*(x)\sin\theta\, e^{\iota\omega t},$$
$$p(x,\theta,t) = P_\infty + p^*(x)\cos\theta\, e^{\iota\omega t}. \quad (24)$$

The equations of continuity and momentum for a incompressible flow may be derived by considering mass and momentum fluxes entering and leaving a small element of the annulus. Neglecting the friction forces on the wall, the governing equation may be written in linear form as

$$\frac{\partial h}{\partial t} + \frac{\partial(hu)}{\partial x} + \frac{1}{r}\frac{\partial(hw)}{\partial\theta} = 0, \quad (25)$$

$$\frac{\partial(\rho hu)}{\partial t} + \frac{\partial}{\partial x}(h(p+\rho u^2)) + \frac{1}{r}\frac{\partial(\rho huw)}{\partial\theta} - P\frac{\partial h}{\partial x} = 0, \quad (26)$$

$$\frac{\partial(\rho hw)}{\partial t} + \frac{1}{r}\frac{\partial}{\partial\theta}(h(p+\rho w^2)) + \frac{\partial(\rho huw)}{\partial x} - P\frac{1}{r}\frac{\partial h}{\partial\theta} = 0, \quad (27)$$

Substitution of equation (24) into the above equations and elimination of the steady flow

equation, $H(\partial U/\partial x) = 0$, gives a set of linear first order differential equations;

$$\frac{du^*}{dx} = -\frac{w^*}{r} - \frac{U}{H}\frac{dE}{dx} - \iota\Omega\frac{E}{H}, \quad (28)$$

$$\frac{dw^*}{dx} = \frac{1}{\rho U}\frac{p^*}{r} - \iota\Omega\frac{w^*}{U}, \quad (29)$$

$$\frac{dp^*}{dx} = -\iota\Omega\rho u^* - \rho U\frac{du^*}{dx}. \quad (30)$$

Considering the normal mode analysis, the solution may be expressed in terms of the eigenfunction of the beam in general. Taking into account the boundary condition shown in equation (16), the nondimensional unsteady velocities and pressure can be separated into trigonometric (s=1) and hyperbolic (s=2) components as follows:

$$\bar{u} = \sum_{k=1}^{n}\sum_{s=1}^{2}(A_{sk}E_{sk}(X) + \iota B_{sk}E_{sk}'(X)),$$

$$\bar{w} = \sum_{k=1}^{n}\sum_{s=1}^{2}(C_{sk}E_{sk}'(X) + \iota D_{sk}E_{sk}(X)),$$

$$\bar{p} = \sum_{k=1}^{n}\sum_{s=1}^{2}(F_{sk}E_{sk}(X) + \iota G_{sk}E_{sk}'(X)), \quad (31)$$

where the prime denotes differentiation with respect to X. Clearly two set of solution arising for trigonometric and hyperbolic components can be associated with E_{1k} and E_{2k} defined in equation (3).

Substituting equation (31) into the governing equations and separating the equations into real and imaginary parts lead to

$$\begin{bmatrix} 1 & 0 & \bar{l} & 0 & 0 & 0 \\ 0 & (-1)^s\beta_k^2 & 0 & \bar{l} & 0 & 0 \\ 0 & 0 & (-1)^{s+1}\beta_k^2 & \omega/U_r & \bar{l} & 0 \\ 0 & 0 & \omega/U_r & 1 & 0 & -\bar{l} \\ 1 & -\omega/U_r & 0 & 0 & 1 & 0 \\ -\omega/U_r & (-1)^{s+1}\beta_k^2 & 0 & 0 & 0 & (-1)^{s+1}\beta_k^2 \end{bmatrix} \begin{Bmatrix} A_{sk} \\ B_{sk} \\ C_{sk} \\ D_{sk} \\ F_{sk} \\ G_{sk} \end{Bmatrix}$$

$$= \begin{Bmatrix} a_k/H \\ \omega a_k/U_r H \\ 0 \\ 0 \\ 0 \\ 0 \end{Bmatrix}, \quad \text{where } \bar{l} = \frac{L}{a + H/2}. \quad (32)$$

By solving the above equation, the coefficients are determined as follows;

$$A_{sk} = \frac{\beta_k^2}{\beta_k^2 + (-1)^{s+1}\bar{l}^2}\frac{a_k}{H},$$

$$B_{sk} = \frac{-1}{\bar{l}^2 + (-1)^{s+1}\beta_k^2}\frac{\omega}{U_r}\frac{a_k}{H}$$

$$C_{sk} = \frac{(-1)^{s+1}}{\beta_k^2}A_{sk}\bar{l} \qquad D_{sk} = -B_{sk}\bar{l},$$

$$F_{sk} = B_{sk}\frac{\omega}{U_r} - A_{sk}$$

$$G_{sk} = A_{sk}\frac{(-1)^{s+1}}{\beta_k^2}\frac{\omega}{U_r} - B_{sk} \quad (33)$$

It ought to be noted that the restriction of the analysis to narrow annuli results in a closed-form solution. Having determined coefficients, the velocities and pressure may be calculated. Proceeding similarly shown in the previous section, the components of fluid forces may be found such that

$$P_{2k} = \sum_{s=1}^{2}Q_{sk}E_{sk}(x) \qquad P_{1k} = 2U\sum_{s=1}^{2}Q_{sk}E_{sk}'(x)$$

$$P_{0k} = -U^2\beta_k^2\sum_{s=1}^{2}(-1)^{s+1}Q_{sk}E_{sk}(x)$$

where

$$Q_{sk} = \frac{1}{[1 + (-1)^{s+1}(\beta_k/\bar{l})^2]H}. \quad (34)$$

Inspecting the above equation, it is clearly shown that the coefficient Q_{sk} depends only on geometry of system and that, as compared to equation (23), the coefficient is equivalent to G_{sk} shown in the numerical method.

3. Method of Stability Analysis

The differential equation of motion of the flexible centre-body together with the boundary condition at both end for a clamped-clamped beam constitutes a boundary value problem. Moreover the boundary conditions are utilized to derive a typical eigenvalue problem. The transition between the boundary value problem and the eigenvalue problem is effected by means of the separation of variables method. The expansion theorem plays a major role in the field of

vibrations and will be used here also to obtain a solution of the system by normal mode analysis.

The solution of the eigenvalue problem is not straightforward as for discrete systems. By using Galerkin's method, however, the system is discretized, leading eventually to the determination of the mass, damping and stiffness matrics of the system. The discretized problem is then easy to solve.

Substituting the nondimensional parameters in equation (5) into the equation (1) of cylinder motion leads to

$$\frac{d^4\eta}{dX^4} + \frac{d^2\eta}{dt^2} = \frac{L^4}{aEI} F_p \tag{35}$$

in nondimensional form. According to Galerkin's method, it is required that the weighted error integrated over domain be zero. The weighted function are the comparison functions E_k defined in equation (3), such that

$$\int_0^1 \left[\frac{d^4E(X)}{dX^4} - \omega^2 E(X) + \sigma P(X)\right] E_j(X)dX = 0,$$
$$j = 1, 2, 3,\ldots\ldots, n,$$

where

$$P(X) = \frac{1}{l^2}[-\omega^2 P_{2k}(X) + \iota\omega P_{1k}(X) + P_{0k}(X)]$$

in which

$$P_{2k}(X) = \sum_{s=1}^{2} G_{sk} E_{sk}(X), \quad P_{1k}(X) = 2U_r \sum_{s=1}^{2} G_{sk} E'_{sk}(X),$$
$$P_{0k}(X) = U_r^2 \beta_k^2 \sum_{s=1}^{2} (-1)^s G_{sk} E_{sk}(X) \tag{37}$$

and j is a dummy index. Of course, for the approximate method, Q_{sk} is used instead of G_{sk} in the above equation. Accordingly, it is possible to express the equation in the form

$$-\omega^2[M]\{A\}e^{i\omega t} + i\omega[C]\{A\}e^{i\omega t} + [K]\{A\}e^{i\omega t} = 0, \tag{38}$$

where the elements of [M], [C] and [K] are given by

$$m_{jk} = \int_0^1 [\, E_k(X) + \sigma P_{2k}(X) \,] E_j(X)\, dX$$

$$c_{jk} = \int_0^1 \sigma P_{1k}(X)\, E_j(X)\, dX \tag{39}$$

$$k_{jk} = \int_0^1 [\, \beta_k^4 E_k(X) + \sigma P_{0k}(X) \,] E_j(X)\, dX$$

and {A} is the vector of the a_k of equation (3). Once equation (38) has been obtained by Galerkin's method, all matrix techniques of a discrete system become available to the solution of the continuous system. In the present analysis, the asymmetry in the matrices [C] and [K] is entirely due to the presence of inviscid fluid-dynamic forces. To allow the determination of the response within the desired accuracy, the present analysis is achieved with five mode approximation (n = 5).

4. Dynamics and Stability

To illustrate the general dynamical behaviour of the system under consideration, typical results are presented. As compared to the basic beam in vacuum, the dynamical behaviour is modified by the fluid-dynamic force, which is a function of the flow velocity. For convenience, the results will be presented in terms of the nondimensional flow velocity, U_n, rather than U. It is of interest to estimate the critical flow velocity in the practical engineering application for design consideration. The dynamical behaviour of the system at higher velocity than this critical threshold is more of an academic interest.

At zero flow velocity, the natural frequencies are obviously dependent on the added mass; fluid-dynamic stiffness and damping coefficients are, of course, to be null. With increasing flow velocity, the frequency of most modes are diminished. For conservative system with clamped ends, the eigenfrequencies remain real with increasing U_n, up to the point of loss of the stability, where the centrifugal force overcomes the flexural restoring force. Here, it is recalled that the system loses stability if $\mathrm{Im}(\omega_n) < 0$, by divergency when $\mathrm{Re}(\omega_n) = 0$ and by flutter when $\mathrm{Re}(\omega_n) \neq 0$.

In general, the lowest critical flow velocity indicating the onset of buckling is approximated by Euler's method of equilibrium[11]. At the buckling onset, the time derivatives in the equation of motion of the centre-body could be eliminated: *i. e.*, the deter-

minant of the stiffness might be zero. As is evident from the equations (23) and (34), the nondimensional critical flow velocity at divergence instability does not depend on the properties but only on the geometry of the system (gap ratio and length ratio). It was noted that the nondimensional critical flow velocity for clamped-clamped beam was estimated easily as the following simple form

$$U_{rl} = \frac{2\pi}{\sqrt{\chi}}, \quad \chi = \frac{(1+H)^2+1}{(1+H)^2-1} \tag{40}$$

based on the slender-body formulation.

The dynamic behaviours of the system obtained by both methods are illustrated in Figure 3, where L/a=20, H/a=0.1, a=323.74 and U_{refl}=1.332 m/s. It is noted that the eigenfrequencies obtained by two methods are similar; the approximate results are sligthly smaller, which reflects the overestimation of fluid effect by the thin film approximation. According to the numerical result based on spectral method, by first mode buckling, the system loses stability at U_{rl}=2.04 (point A in the diagram) where changes from purely real to purely imaginary and one branch of the bifurcated locus on the Im(ω_n)-axis is negative. But the system regains stability in its first mode at U_{rl}=3.08 (point B). At slightly higher flow velocity, the loci of the first and second modes coalesce on the Re(ω_n)-axis and becomes complex, indicating the onset of the coupled-mode flutter at U_{rl}=3.37 (point C). Interestingly, this behaviour was suggested to be related to the well-known gyroscopic forces; *e. g.*, in connection with the whirling of shaft[13]. These symmetric coupled-modes, with respect to Re(ω_n)-axis, bifurcated on the Re(ω_n)-axis at D where the system regains stability. The regions associated with higher flow velocity are quite complex.

The influence of the number of the collocation point, m, on the accuracy of the present spectral method is shown in Table 1. With increasing the number, it is found that the numerical results are exponentially converged. In order to obtain the same accuracy for larger H/a, a smalll increase in the number is to be needed.

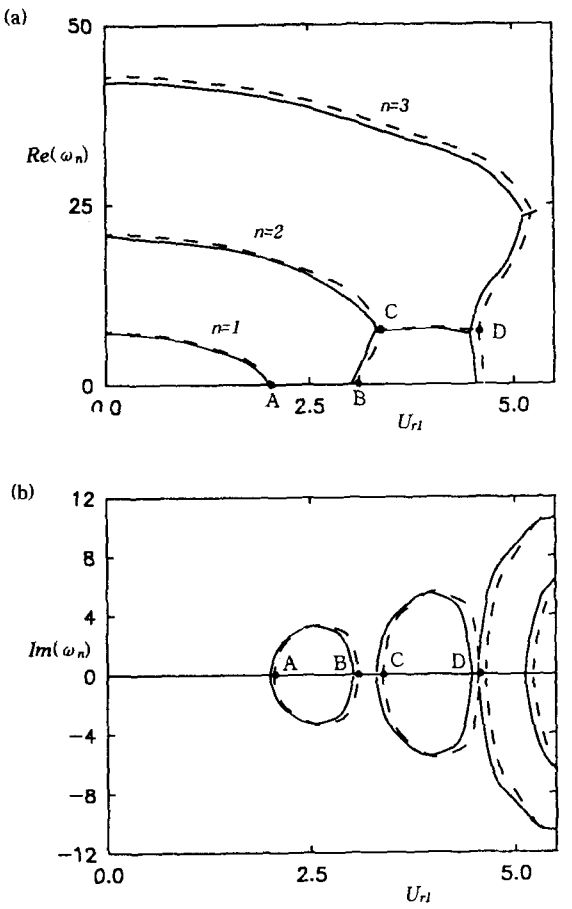

Fig. 3. The Nondimensional Eigenfrequencies of the Lowest Three Modes as Function of the Nondimensional Fluid Velocity, U_{rl}, Calculated by Numerical Method (- - - -) and by Analytical Method (——): (a) the Real Components (b) Imaginary Components (L/a=20, H/a=0.1, σ=323.74 and U_{refl}=1.332 m/s)

The effect of varying the relative gap H/a on the dynamical behaviour of rubber-air system is shown in Figure 4 for L/a=20, σ=0.425 and U_{refl}=36.77 m/s. The results are obtained by numerical method: CFD solution. Here, the first and second modes appear to buckle at A and B. As contrast to the results shown in Figure 3, the frequency of the second

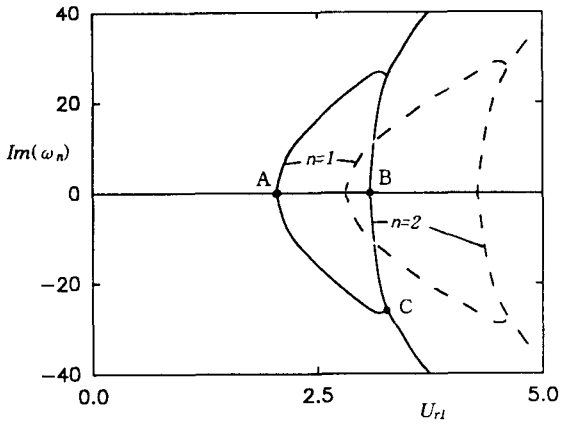

Fig. 4. The effect of Varying Annular Gap, H/a, on the Imaginary Components of the Nondimensional Eigenfrequenies of the Lowest Two modes as Function of the Nondimensional Fluid Velocity, U_{rl} (L/a=20, σ=0.425 and U_{refl}=36.77 m/s)
—— H/a=0.1, ---- H/a=0.2

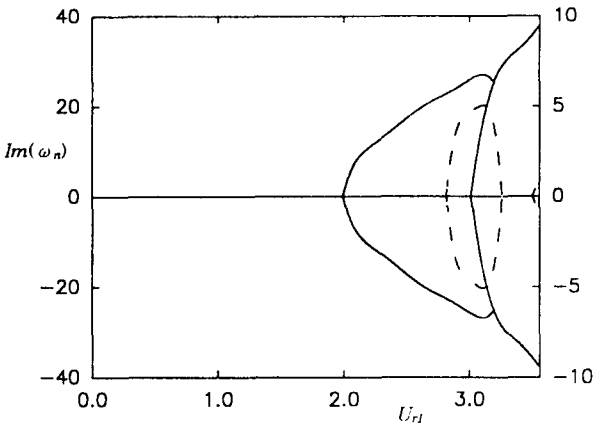

Fig. 5. The effect of Varying Length-to-radius Ratio, L/a, on the Imaginary Components of the Nondimensional Eigenfrequenies of the Lowest Two modes as Function of the Nondimensional Fluid Velocity, Ur1 (H/a=0.1): Left Label for L/a=20, Right Label for L/a=10.
---- L/a=10 σ=0.106 and U_{refl}=73.54 m/s
—— L/a=20 σ=0.425 and U_{refl}=36.77 m/s

Table 1. The Variation of the nondimensional critical flow velocity, U_{rl}, with the collocation points, m.

		m=3	m=4	m=5	m=7	m=10
U_{rl} (PD*%)	L/a=22, H/a=0.05	1.500 (3.67)	1.446 (0.07)	1.447	1.447	1.447
	L/a=22, H/a=0.20	3.270 (16.95)	2.769 (0.97)	2.799 (0.11)	2.796	2.796
	L/a=22, H/a=0.40	5.339 (41.69)	3.619 (3.95)	3.795 (0.72)	3.769 (0.03)	3.768
	L/a=38, H/a=0.40	5.201 (42.65)	3.502 (3.95)	3.672 (0.71)	3.646	3.646

* Note: Percent discrepancy based on the last column (m=10).

mode vanish at B, indicating the onset of buckling in its mode and then the loci of the first and second modes coalesce on the $Im(\omega_n)$-axis and leave the axis at symmetric points C indicating the onset of coupled-flutter. To show the effect of the length-to-radius ratio on the dynamical behaviour of system, the imaginary component of the eigenfrequency versus nondimensional flow velocity, given by the approximate analytical method, is presented in Figure 5 for L/a=10, H/a=0.1, σ=0.106 & U_{refl}=73.54 m/s and for L/a=20, H/a=0.1, σ=0.425 & U_{refl}=36.77 m/s. It is clearly shown that the nondimensional critical flow velocity becomes higher with decreasing the length-to-radius ratio. In Figure 6, the critical flow velocities caused by buckling in the first mode versus annular gap are illustrated for rubber-air and rubber-water systems with two different length-to-radius ratios (L/a=30 & 38). It was found that the nondimensional critical flow velocity obtained by potential theory does not depend on fluid properties but only on the geometry of system as discussed before. In general, it has been known that hydrodynamic or 'virtual' mass becomes large with decreasing the annular gap for confined flow.

It is also of interest to compare these critical velocities estimated by the present theory with those

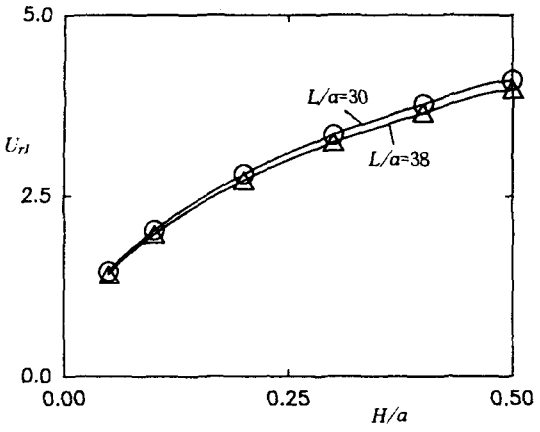

Fig. 6. The Nondimensional Critical Flow Velocity versus Annular Gap H/a, by Buckling in the first Mode for Robber-air System(——) and Rubber -water System(△, ○) with two Different Length-to-radius Ratios(L/a=30 & 38).

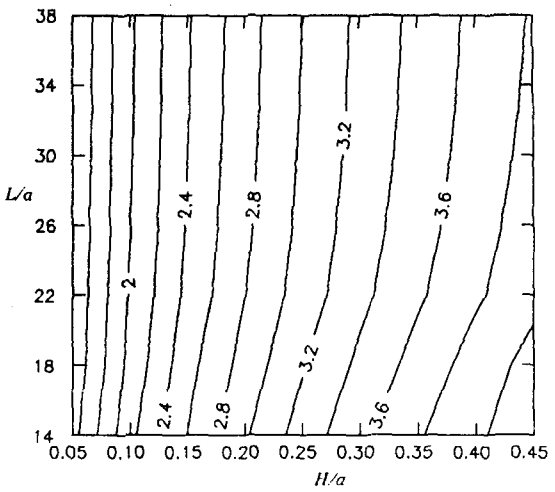

Fig. 7. The Contour Map Showing the Variation of the Nodimensional Critical Flow Velocity, U_{r1}, in the First Mode Buckling with Respect to Length-to-radius Ratio and Annular Gap-to-radius Ratio for Rubber-air System.

Table 2. Comparison of the nondimensional critical flow velocity, U_{r1}, obtained with present and earlier theories.

L/a	H/a	Previous Theory		Present Theory	
		(1)	(2)	Appr.	CFD
20	0.05	1.39	1.49	1.44	1.46
	0.10	1.94	2.13	1.99	2.04
	0.15	2.34	2.64	2.39	2.47
100	0.01	0.627	0.631	0.627	0.628
	0.05	1.387	1.425	1.374	1.391

Note: (1) Slender Body Theory[11]
(2) Narrow Annular Flow Theory[9]

obtained by previous methods(slender body theory[11] and Narrow annular flow theory[9]); this comparison is shown in Table 2. Satisfaction, in quantitative agreement of critical flow velocity, is found. It is seen that the best agreement is for a very slender body (L/a=100), where slender-body theory applies best, and for a very narrow annulus (H/a=0.01), where the narrow-annulus simplication also applies best.

A contour map is illustrated in Figure 7 for rubber-air system to show the variation of the nondimensional critical flow velocity, U_{r1}, versus length -to-radius ratio and annular gap-to-radius ratio: e. g., the system loses stability by buckling in its first mode at 2.88 of the nondimensional flow velocity for L/a=18 and H/a=0.2. As discussed before, the nondimensional critical flow velocity becomes high with increasing the annular gap and decreasing the length-to-radius ratio. This map might be very useful in the practical engineering application for design consideration.

Finally, from the above results, it is noted that the system with the lowest density fluid and/or the shortest length of cylinder requires a much higher dimensional flow velocity to cause instability-which is considered reasonable; however, the nondimensional critical flow velocity is kept the same.

5. Conclusions and Discussion

A new numerical model based on spectral method has been developed for studying the dynamics and stability of flexible cylinder in a duct with inviscid annular flow. The method was used to estimate the critical flow velocity, where system loses stability, more rigorously. One of the main contributions of the present work is to develop a numerical mothod which is applicable to the system having relatively wide annular gap and/or short length of cylinder, as compared to existing theory. The developed method was validated by comparing its results with those of the present analytical method based on thin film approximation, especially for short length of cylinder; in this case, an available model does not exist. Recent analytical studies on the flow-induced vibration problem shows that the viscous effect on the fluid-dynamic force can be negligible for relatively high oscillatory Reynold number or/and wide annular gap. Thus, the viscous effect has been excluded in the present work.

The results of spectral collocation method shows that the prediction of inviscid hydrodynamic force is quite different and superior to that of previous theory. In the present numerical theory, instead of obtaining the unsteady force by an adaptation of formualtions applicable to slender body and/or narrow annular flow, they are derived numerically by means of full Laplace equation without simplification.

Based on the inviscid theory, it is noted that the dynamical behaviour of the system is similar to that of system with unconfined flow or with internal flow. Some general but important conclusions, for inviscid flow, are presented here, as follows:

(a) the flexible centre-body with fixed both ends becomes unstable by first-mode buckling.

(b) the nondimensional critical flow velocity depends only on the geometry of system,

(c) the dimensional critical flow velocity becomes smaller as the annular gap becomes narrower and as the fluid has larger density.

(d) the characteristic of the system after the onset of buckling in its first mode depends on the Coriolis force.

In the present analysis, both ends of the flexible centre-body are supposed to be clamped. Thus it is needed to investgate the dynamics and stability of other systems having different boundary conditions; *e. g.*, clamped-free or pinned-pinned beams. Also to examine the present results, it is obviously necessary to carry out experimental test. Since the viscous effect on the dynamical behaviour of system becomes no more negligible specially for narrow annular configuration, it is required to modify the present spectral theory. An attempt should be made to extend the present numerical method for studying the viscous effects on the dynamical behaviour of system, which we are pursuing as the next investigation.

References

1. Mulcahy, T. M., "A Review of Leakage-Flow-Induced Vibration of Reactor Components", Argonne National Laboratory Report, ANL−83−43 (1983).
2. Chen, S. S., Wambsgannss, M.W. and Jendrzejczyk, A. Z., "Added Mass and Damping of a Vibrating Rod in Confined Viscous Fluid", Journal of Applied Mechanics, Vol. 43, pp. 325−329 (1976).
3. Gorman, D.J., Godon, J.L. and Planchard, J., "Analytical and Experimental Study of the Vibratory Response of a Flexible Tube Subjected to External Annular Flow Part Way along its Length", In Proceedings BHRA Conference on Flow-Induced Vibration (ed. R. King), Bowness-on-Windermere, UK. Cranfield: BHRA (1987).
4. Paidousiss, M. P., "Flow-induced Vibration Problems in Nuclear Reactors and Heat Exchangers: Practical Experiences and State of Knowledge", In Proceeding IAHR-IUTAM Symposium on Practical Experiences with Flow-induced Vibrations, Karlsruhe (eds E. Naudascher

and D. Rockwell), pp. 1−81, Berlin : Springer-Verlag (1980).

5. Mateescu, D., Paidoussis, M.P. and Sim, W.−G., "A Spectral Collocation Method for Confined Unsteady Flows with Oscillating Boundaries", Journal of Fluids and Structures, Vol. 8, pp. 157-181 (1994).
6. Hobson, D. E., "Fluid-Elastic Instabilities Caused by Flow in an Annulus", Third International Conference on Vibration in Nuclear Plant, Keswick, UK (1982).
7. Mateescu, D. and Paidoussis, M. P., "The Unsteady Potential Flow in an Axially Variable Annulus and its Effect on the Dynamics of the Oscillating Rigid Centre-Body", ASME Journal of Fluids Engineering, Vol. 107, pp. 421−427 (1985).
8. Mateescu, D. and Paidoussis, M. P., "Unsteady Viscous Effects on the Annular-Flow-Induced Instabilities of a Rigid Cylindrical Body in a Narrow Duct", Journal of Fluids and Structures, Vol. 1, pp. 197−215 (1987).
9. Paidoussis, M. P., Mateescu, D. and W.−G., Sim, "Dynamics and Stability of a Flexible Cylinder in a Narrow Coaxial Cylindrical Duct Subjected to Annular Flow", Journal of Applied Mechanics, Vol. 57, pp. 232−240 (1990).
10. Mateescu, D., Paidoussis, M.P. and Sim, W.−G., "Spectral Solutions for Unsteady Annular Flows Between Eccentric Cylinders Induced by Transverse Oscillations", Accepted for Publication in Journal of Sound and Vibration, (1994).
11. Paidoussis, M. P., "Dynamics of Cylindrical Structure Subjected to Axial Flow", Journal of Sound and Vibration, Vol. 29, pp. 365−385 (1973).
12. Paidoussis, M.P. and Issid, N. T., "Dynamics Stability of Pipes Conveying Fluid", Journal of Sound and Vibration, Vol. 33, pp. 267−294 (1974).
13. Meirovich, L., Methods of Analytical Dynamics, Chapter 4, Mcgraw-Hill, New York (1983).